Gas Sensors Hot Paper

International Edition: DOI: 10.1002/anie.201707491
German Edition: DOI: 10.1002/ange.201707491

Bio-Inspired Carbon Monoxide Sensors with Voltage-Activated Sensitivity

*Suchol Savagatrup[+], Vera Schroeder[+], Xin He, Sibo Lin, Maggie He, Omar Yassine, Khaled N. Salama, Xi-Xiang Zhang, and Timothy M. Swager**

Abstract: *Carbon monoxide (CO) outcompetes oxygen when binding to the iron center of hemeproteins, leading to a reduction in blood oxygen level and acute poisoning. Harvesting the strong specific interaction between CO and the iron porphyrin provides a highly selective and customizable sensor. We report the development of chemiresistive sensors with voltage-activated sensitivity for the detection of CO comprising iron porphyrin and functionalized single-walled carbon nanotubes (F-SWCNTs). Modulation of the gate voltage offers a predicted extra dimension for sensing. Specifically, the sensors show a significant increase in sensitivity toward CO when negative gate voltage is applied. The dosimetric sensors are selective to ppm levels of CO and functional in air. UV/Vis spectroscopy, differential pulse voltammetry, and density functional theory reveal that the in situ reduction of Fe^{III} to Fe^{II} enhances the interaction between the F-SWCNTs and CO. Our results illustrate a new mode of sensors wherein redox active recognition units are voltage-activated to give enhanced and highly specific responses.*

Carbon monoxide (CO) is responsible for more than half of all fatal poisonings worldwide.[1] Exposure to the colorless, tasteless, and odorless gas is difficult to discern as the initial symptoms of poisoning (headache, dizziness, and confusion) are nonspecific. In the United States, the Occupational Safety and Health Administration (OSHA) has designated permissible exposure limits of 50 ppm over eight hours and 200 ppm over five minutes.[2] The affinity of iron porphyrin towards CO is well-documented for the enzymes cytochrome P450,[3–5] hemoglobin,[6] and myoglobin.[7] This high affinity for CO over O_2 of hemoglobin and myoglobin is the underlying mechanism of carbon monoxide poisoning in mammals.[8,9] Although detectors for CO are available, there remains a need for massively distributed sensors that are small and inexpensive to prevent poisoning in domestic and industrial environments. Single-walled carbon nanotube (SWCNT) chemiresistors and chemical field effect transistors (ChemFET) have been shown to provide suitable platforms for the detection of various gases.[10–15] Random networks of functionalized SWCNTs have produced sensors that are inexpensive to fabricate, operate at room temperature, and have ultra-low power requirements.[16,17] Theoretical and experimental reports have suggested that CO does not engage in charge transfer with pristine SWCNTs,[18–20] indicating that a chemical reactive interface is necessary. Conductivity-based CO detection has been reported for carboxylate-containing,[19] deformed,[21] or doped SWCNTs,[22] as well as SWCNTs dispersed in polymers[23] or decorated with metallic nanoparticles.[24] Alternatively, non-chemiresistive examples of SWCNT CO detectors rely on other mechanisms including changes in capacitance[25] and resonant frequency.[26]

Although as summarized CO detectors based on SWCNTs have been reported, none make use of an in situ activated selector to produce additional selectivity and sensitivity. Previously, our group reported a chemiresistive sensor using an organocobalt complex to bind CO.[27] The cobalt selector demonstrated exceptional selectivity in air; however, the mechanism of detection required mobility of the complex which was provided by a fluid matrix and the lowest experimentally detected concentration was 800 ppm. Dong et al. have reported heme-modified chromium electrodes capable of CO detection in N_2, but device-to-device reproducibility, selectivity, and air stability were not reported.[28] Even with these successful examples, the responsivity of the selectors cannot be controlled externally, which may limit the functionality of the sensors.

A selector with a predictive modulated responsivity enables extraction of more information from a single sensor element. To this effect, we designed CO detectors comprising pyridyl-functionalized SWCNTs as the matrix and bio-inspired iron porphyrin, a core element of many metalloenzymes/proteins,[29–32] as a selector that can be activated and deactivated by modifying the gate voltage (Figure 1). Fe^{III} porphyrin is the persistent state in ambient atmosphere, however only the air sensitive Fe^{II} binds CO. As a result, we reasoned that an applied gate voltage can transiently reduce the iron porphyrin in situ from Fe^{III} to Fe^{II} and thus enable CO binding. The redox equilibration between SWCNTs and a Fe^{II} porphyrin and the prospects for detecting CO have been

[*] S. Savagatrup,[+] V. Schroeder,[+] S. Lin, M. He, T. M. Swager
Department of Chemistry and Institute for Soldier Nanotechnologies, Massachusetts Institute of Technology, 77 Massachusetts Avenue
Cambridge Massachusetts 02139 (USA)
E-mail: tswager@mit.edu

X. He, X.-X. Zhang
Physical Science and Engineering Division
King Abdullah University of Science and Technology, KAUST
Thuwal 23955-6900 (Saudi Arabia)

O. Yassine, K. N. Salama
Sensors Lab, Computer, Electrical and Mathematical Science and Engineering Division
King Abdullah University of Science and Technology, KAUST
Thuwal 23955-6900 (Saudi Arabia)

[+] These authors contributed equally to this work.

Supporting information and the ORCID identification number(s) for the author(s) of this article can be found under: https://doi.org/10.1002/anie.201707491.

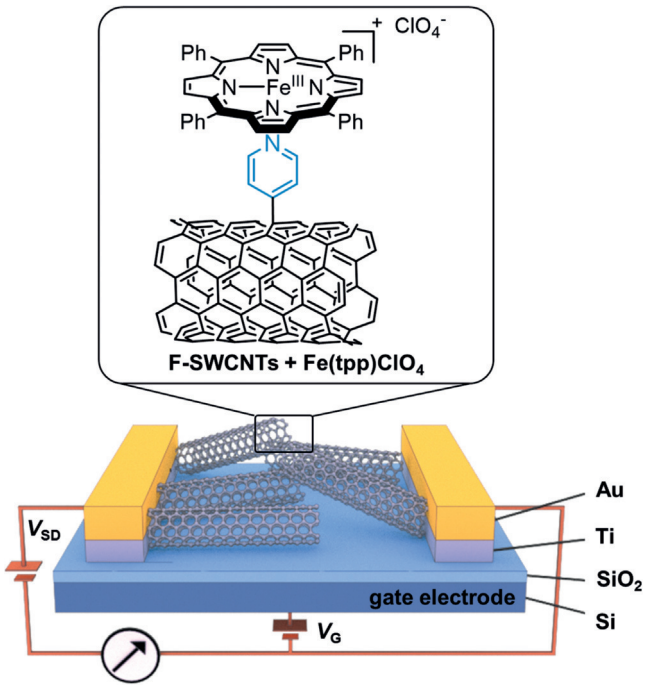

Figure 1. Carbon monoxide detection by a bio-inspired sensor. Schematic of a field-effect transistor (FET) substrate with Au source-drain electrodes and Ti adhesion layer deposited on SiO_2 dielectric layer and Si gate electrode. Chemical structures of pyridyl-functionalized single-walled carbon nanotubes (F-SWCNTs) and iron porphyrin (Fe-(tpp)ClO_4), depicting the coordination chemistry of the pyridyl group to the iron center of the porphyrin.

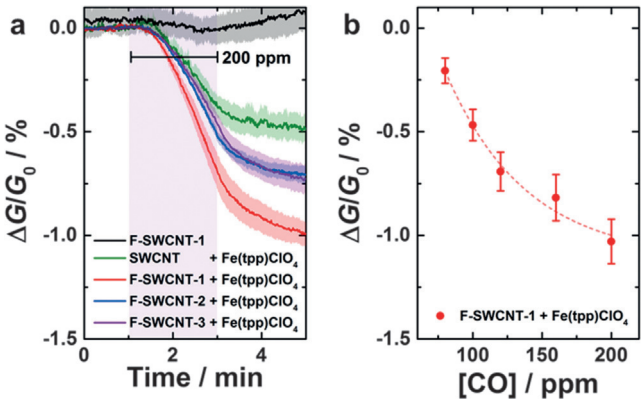

Figure 2. Sensing responses at no gate voltages. a) Average changes in the conductance and standard deviations ($N \geq 6$ sensors) in response to 2 min exposures to 200 ppm of CO for F-SWCNTs without Fe(tpp)ClO_4 (black), pristine SWCNTs with Fe(tpp)ClO_4 (green), and three densities of functionalization (red, blue, violet). b) Conductance changes of **F-SWCNT-1** with Fe(tpp)ClO_4 in response to various concentrations of CO gas diluted in N_2.

analyzed computationally, for a system comprising two SWCNTs covalently linked via an iron(II) porphyrin.[33] Additionally, iron porphyrin-based CO detection schemes have been investigated in biological systems.[34] We have applied a recently developed scheme for iodonium functionalization to precisely attach single aromatic rings to the sidewalls of SWCNTs.[35] This method allows us to confidently install a pyridyl group attached in the 4 position to the SWCNT for anchoring of the 5,10,15,20-tetraphenyl-porphyrin iron(III) perchlorate (Fe(tpp)ClO_4) that serves as our redox active CO binding site.

In developing an optimal sensor, the density of the CO binding and transducing sites is critical. We controlled the density of pyridyl groups on the SWCNTs by the ratio of pristine SWCNTs to sodium naphthalide and pyridyl iodonium salt during synthesis (Figure S2 in the Supporting Information). Using a ratio of 1:0.05:0.05 equivalents of pristine SWCNTs, sodium naphthalide, and iodonium salt, respectively,[35] we obtained 1.4 pyridyl groups per 100 SWCNT carbon atoms (**F-SWCNT-1**). ^{1}H NMR analysis of the post-functionalization filtrate confirmed that the pyridyl groups were the dominant functional group on the SWCNTs (Figure S4). Doubling the amount of sodium naphthalide and iodonium salt in relation to the pristine SWCNTs increased the pyridyl concentration to 1.9 per every 100 SWCNT carbon atoms (**F-SWCNT-2**). Further doubling of the two reactants only resulted in a small increase of functionalization of 2.0 per 100 SWCNT carbon atoms (**F-SWCNT-3**). Figure 2a shows the average change in conductance normalized to the initial conductance ($\Delta G/G_0$) of sensors with the different levels of functionalization in response to 2 min exposures of 200 ppm CO after a linear baseline correction. This post-acquisition data processing was used to mitigate the slight drift in the conductance of the sensors. Sensors without iron porphyrin-both pristine (not shown) and functionalized (black curve) SWCNTs-showed negligible responses to CO, which was consistent with the previous reports.[18–20,27]

Sensors with iron porphyrin showed dosimetric responses indicating irreversibility over the experimental time frame. Pristine SWCNTs (lacking the 4-pyridyl anchor group) when treated with Fe(tpp)ClO_4 (green curve) showed a modest response (-0.57 ± 0.09 %). The response increased significantly with the introduction of sidewall pyridyl groups in **F-SWCNT-1** (-1.08 ± 0.05 %). We hypothesize that the increase of the signal reflects improved electronic communication and special organization of the SWCNTs and Fe(tpp)ClO_4. Differential pulse voltammetry (DPV) of pristine SWCNTs and **F-SWCNT-1** treated with Fe(tpp)ClO_4 confirmed that the pyridyl groups facilitates electron transfer to the Fe center (Figure S6). The decrease in conductance upon exposure to CO is consistent with the sensors comprising a *p*-type polymer and iron porphyrin reported by Paul et al.[36] Additionally, the observed decrease in conductivity of the sensors is consistent with the DFT prediction by Zhao and co-workers.[33]

Higher densities of pyridyl groups (**F-SWCNT-2** and **F-SWCNT-3**) produced decreased responses (blue and purple curves), suggesting that a detrimental perturbation of the SWCNT sp^2 networks occurred with high levels of covalent functionalization.[37–39] As shown in the Ultraviolet-visible-near infrared (UV/Vis-NIR) spectra (Figure S3d), the disappearance of the Van Hove transitions in **F-SWCNT-2** and **F-SWCNT-3** verified the degraded extended electronic structures of the SWCNTs. This result highlights the importance of balancing the degree of functionalization and preserving the native characteristics of the SWCNT.

To evaluate the real-world applicability of our sensors, we have investigated their sensitivity and selectivity. Figure 2b summarizes the responses to various concentrations of CO. The lowest detected concentration was 80 ppm of CO in N_2, well within the range of industry standards for CO detectors (Table S3) and the OSHA limit of 200 ppm during a 5 min period.[2] As a result of the irreversibility of our sensors, lower concentrations can be detected at longer exposure times. We have further determined that our CO sensors give robust responses in humid air (42% relative humidity) (Figure 3a). Figure 3b shows the responses to CO compared to CO_2 and O_2. The sensors have negligible responses to 8000 ppm CO_2 (-0.08 ± 0.04%). For O_2 at 8000 ppm (ambient atmosphere is 209,500 ppm O_2), we observed a moderate response (-0.48 ± 0.03%). These findings reflected the relative binding strengths between iron porphyrin and selected small molecules ($CO > O_2 > CO_2$).[40–42] The fact that CO outcompetes the binding of O_2 allows our sensor to operate under ambient conditions.

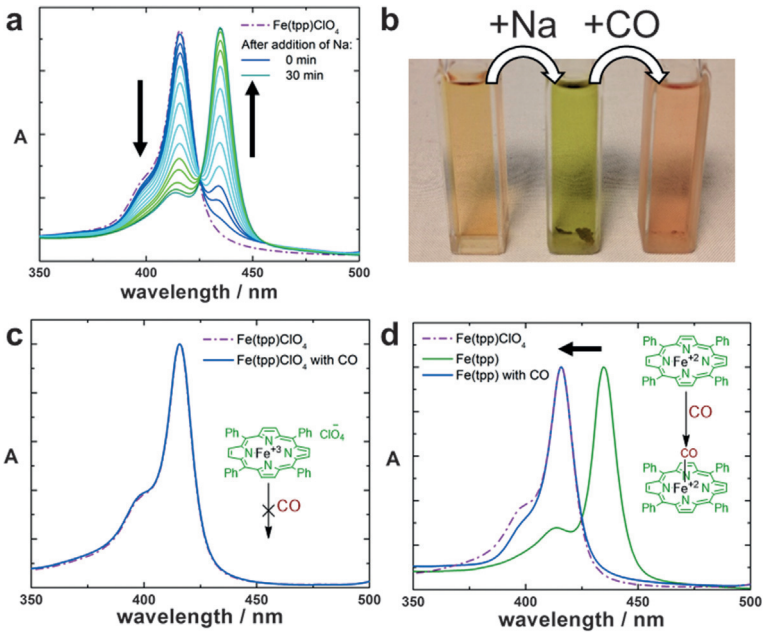

Figure 4. UV/Vis investigation of reactivity of $Fe(tpp)ClO_4$ to CO in solution of THF. a) $Fe(tpp)ClO_4$ before and at various times after addition of Na metal. b) Photograph of the color change with the addition of sodium metal and subsequent addition of carbon monoxide. c) Non-reduced $Fe(tpp)ClO_4$ before and after addition of CO. d) Blue shift in the spectra of fully reduced porphyrin upon addition of CO.

To verify that the sensing mechanism arises from the interaction between CO and iron(II) porphyrin, we performed parallel solution studies.[43] $Fe^{III}(tpp)ClO_4$ can be chemically reduced to $Fe^{II}(tpp)$ in THF solution using Na metal; in the UV/Vis, this change is observed as a red shift of $\Delta\lambda = 16$ nm (Figure 4a and b). The reduced species is moderately stable towards re-oxidation in air (Figure S9a). Addition of CO to a THF solution of $Fe^{III}(tpp)ClO_4$ (Figure 4c) produces no response, whereas $Fe^{II}(tpp)$ reacts quickly with CO as evidenced in a blue shift of $\Delta\lambda = 16$ nm (Figure 4b and 4d).[34] We note here that this shift was stable after the removal of CO (Figure S9b), which is consistent with the irreversible binding of CO to the porphyrin. Our spectroscopic studies are in line with previous solution studies of CO binding to porphyrins.[44] Additionally, DPV of the composite of **F-SWCNT-1** and iron porphyrin showed a decrease in intensity of the reduction peak from Fe^{III} to Fe^{II} when exposed to CO (Figure S6). We ascribed this observation to the fact that CO attenuates the re-oxidation of Fe^{II}.[45] These findings support our hypothesis that in situ reduction of the iron porphyrin will provide for increased sensor response due to a stronger interaction with CO.

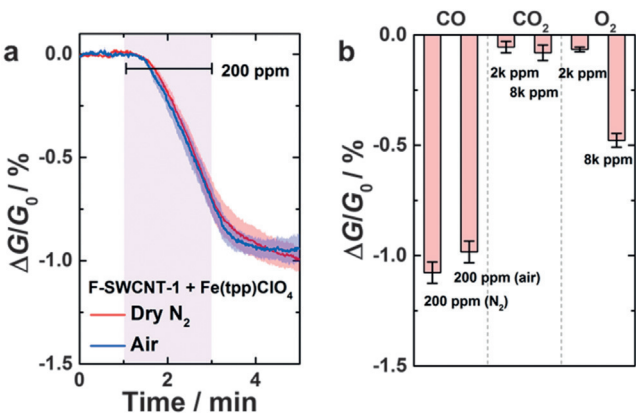

Figure 3. Robustness and selectivity of the CO sensors. a) Conductance curves of **F-SWCNT-1** with $Fe(tpp)ClO_4$ sensors in response to 2 min of 200 ppm of CO gas in air (42% relative humidity) and dry N_2. b) Comparison between the response to CO in both N_2 and air to the responses to CO_2 and O_2.

Having established the chemiresistive behavior, we then investigated the effect of the applied gate voltage on the responsiveness of our sensors. We expected based on our UV/Vis and DPV investigations that the application of the gate voltage would affect the redox state of the iron porphyrin. Figure 5a shows the average change in conductance of the sensors with the applied gate voltage of −3, 0, and 3 V when exposed to 200 ppm CO. Figure 5b summarizes the change in conductance upon exposure to CO as a function of the applied gate voltage. At a gate voltage of −3 V, the response increased to -1.96 ± 0.16%, nearly doubling the response at $V_G = 0$. The response towards CO strongly increased upon the application of negative gate voltage and decreased upon the application of a positive gate voltage. We have determined that the semiconducting nature of **F-SWCNT-1** is not responsible for this behavior as both the **F-SWCNT-1** with and without $Fe^{III}(tpp)ClO_4$ (and P-SWCNTs) display metallic transfer characteristics (Figure S13). UV/Vis spectroscopy revealed that the iron porphyrin was partially reduced by the SWCNTs when initially deposited on the sensors (Figure S9c). This accounts for the enhanced sensitivity with the addition of $Fe^{III}(tpp)ClO_4$ and the attenuation of the response to CO under positive gate voltage. Inversely, the application of a negative gate voltage reduces the porphyrin in situ thereby increasing the affinity towards CO, the electron

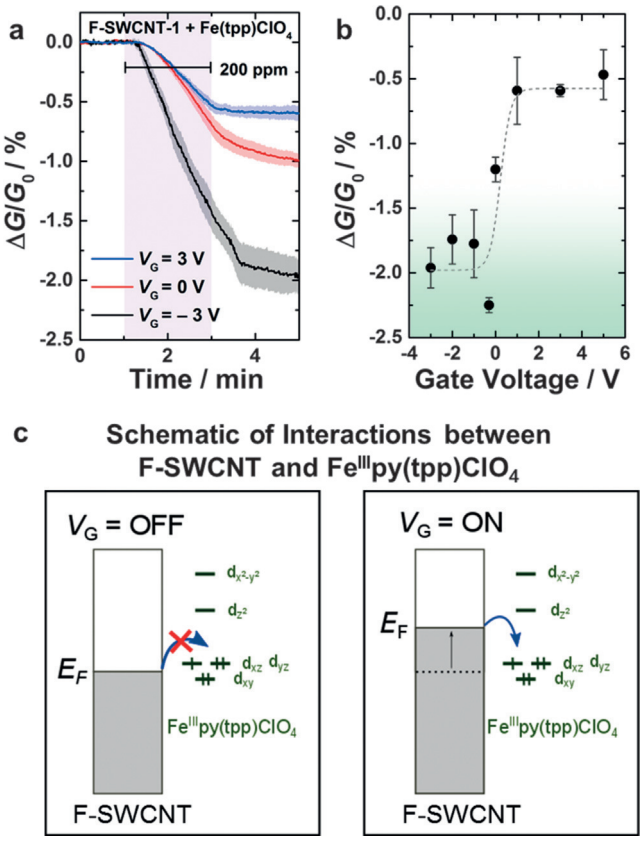

Figure 5. Enhancement in sensitivity via the application of the gate voltage. a) Conductance curves of **F-SWCNT-1** with Fe(tpp)ClO_4 sensors in response to 2 min of 200 ppm of CO at +3, 0, and −3 V gate voltage. b) Change in conductance towards an exposure of 2 min at 200 ppm of CO as a function of the gate voltage. Dashed line to guide the eye. c) Schematic of band diagram of SWCNT and Fe^{III}py(tpp)ClO_4 (py = pyridine) and interactions between the two upon application of gate voltage.

accepting ligand. We attributed the mechanism to a change in the Fermi energy level of the F-SWCNTs with applied gate voltage that then increases the proportion of reduced iron porphyrin. Figure 5c schematically illustrates the in situ reduction of Fe^{III} to Fe^{II} with a change in the SWCNT Fermi level. Hence, we achieve a stronger interaction between the Fe^{II} center and the σ-donating, π-accepting CO ligand.

To gain further insights into the sensing mechanism, we performed density functional theory (DFT) calculations on a SWCNT fragment with Fe^{II} porphyrin in the presence and absence of small gaseous ligands (O_2 and CO). We chose to model a fragment of (5,5) SWCNT containing 110 carbon atoms end-capped with hydrogen atoms for comparison to established procedures.[46–48] This approach is similar to that used by Zanolli et al. who used the computed location of the Fermi level to illuminate the sensing behaviors of a gold-decorated SWCNT.[46] The ground-state geometries, computed distance between the SWCNT and Fe, the bond lengths between Fe and the ligands, binding angles between Fe and the ligands, and the charge transfer between SWCNT and porphyrin are shown in Figure S10 and Table S4. Figure 6 shows the change in computed Fermi energy (ΔE_f) upon adsorption of Fe^{II} porphyrin to a (5,5) SWCNT fragment and the subsequent binding of CO or O_2. The adsorption of Fe^{II} porphyrin increased the Fermi level by 0.12 eV. Binding of CO and O_2 both reduced the Fermi level by 0.19 eV and 0.04 eV, respectively. Consistent with our sensing results, the binding of CO induced a more pronounced change when compared to the binding of O_2. This computed change in Fermi energy is in line with the trends of the sensing data and the decrease in conductance upon binding of CO and O_2. Although other sensing mechanisms have been reported, such as swelling of the SWCNT network or the junctions between electrode and SWCNT, electron transfer has been shown as the dominant factor in the majority of porphyrin-based SWCNT sensors.[13,44,49]

In conclusion, we developed an amperometric platform for the detection of CO with voltage-modulated sensitivity using the bio-inspired interaction between CO and iron porphyrin. We demonstrated the importance of installing covalent pyridyl ligands on the SWCNTs for localizing and electronically coupling the iron porphyrins to the carbon nanotubes. We further demonstrated that the application of the gate voltage can significantly enhance the sensitivity of the sensors and showed that this enhancement can be understood as a result from an increase of Fe^{II} porphyrin species. Our sensors function in oxygenated and humid conditions and have sensitivities to meet the limits of detection required by OSHA. While we are competitive in terms of sensitivity and response time with commercial sensors, we did not pursue optimizations in this current report. The concept of using gate modulated redox states of receptors/selectors attached to SWCNTs is likely to have

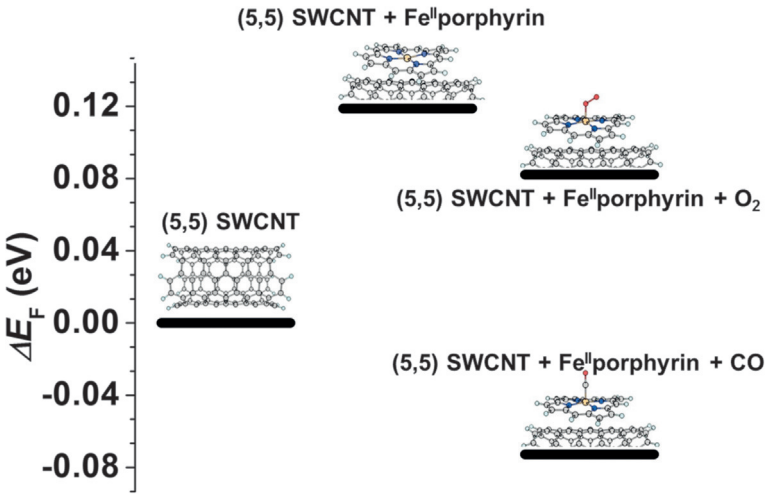

Figure 6. Computed change in the Fermi energy (ΔE_F) upon addition of Fe^{II} porphyrin and subsequent addition of CO or O_2 relative to the Fermi energy of the pristine SWCNT with inserts of the ground-state geometries. For these molecules the Fermi level is defined as the level of the HOMO.

general applicability and we are seeking to demonstrate similarly selective sensors for other analytes.

Acknowledgements

This work was supported by the KAUST sensor project CRF-2015-SENSORS-2719 and the Army Research Office through the Institute for Soldier Nanotechnologies and the National Science Foundation (DMR-1410718). S.L. was supported by an F32 Ruth L. Kirschstein National Research Service Award. M.H. was supported by NIH Training Grant T32ES007020. We thank Dr. Lionel Moh for the designs of the substrates for our sensors and Dr. Joseph Walish for fabricating the gas enclosures.

Conflict of interest

The authors declare the following competing financial interest(s): A patent has been filed on this technology.

Keywords: Carbon monoxide · carbon nanotubes · iron porphyrin · sensors · voltage-activated

How to cite: *Angew. Chem. Int. Ed.* **2017**, *56*, 14066–14070
Angew. Chem. **2017**, *129*, 14254–14258

[1] J. A. Raub, M. Mathieu-Nolf, N. B. Hampson, S. R. Thom, *Toxicology* **2000**, *145*, 1–14.
[2] Occupational Safety and Health Administration, "Carbon Monoxide In Workplace Atmospheres (Direct-Reading Monitor)," **1993**.
[3] F. J. Gonzales, *Pharmacol. Rev.* **1985**, *40*, 243–288.
[4] M. Klingenberg, *Arch. Biochem. Biophys.* **1958**, *75*, 376–386.
[5] T. Omura, R. Sato, *J. Biol. Chem.* **1964**, *239*, 2370–2378.
[6] M. F. Perutz, *Annu. Rev. Physiol.* **1990**, *52*, 1–25.
[7] A. Rossi-Fanelli, E. Antonini, *Arch. Biochem. Biophys.* **1958**, *77*, 478–492.
[8] S. R. Thom, *N. Engl. J. Med.* **2002**, *347*, 1105–1106.
[9] S. R. Thom, L. W. Keim, *Clin. Toxicol.* **1989**, *27*, 141–156.
[10] J. F. Fennell Jr., S. F. Liu, J. M. Azzarelli, J. G. Weis, S. Rochat, K. A. Mirica, J. B. Ravnsbæk, T. M. Swager, *Angew. Chem. Int. Ed.* **2016**, *55*, 1266; *Angew. Chem.* **2016**, *128*, 1286.
[11] J. E. Ellis, A. Star, *ChemPlusChem* **2016**, *81*, 1248–1265.
[12] L. Torsi, M. Magliulo, K. Manoli, G. Palazzo, *Chem. Soc. Rev.* **2013**, *42*, 8612–8628.
[13] S. F. Liu, A. R. Petty, G. T. Sazama, T. M. Swager, *Angew. Chem. Int. Ed.* **2015**, *54*, 6554; *Angew. Chem.* **2015**, *127*, 6654–6557.
[14] A. Star, J. C. P. Gabriel, K. Bradley, G. Grüner, *Nano Lett.* **2003**, *3*, 459–463.
[15] R. P. Deo, J. Wang, I. Block, A. Mulchandani, K. A. Joshi, M. Trojanowicz, F. Scholz, W. Chen, Y. Lin, *Anal. Chim. Acta* **2005**, *530*, 185–189.
[16] B. Esser, J. M. Schnorr, T. M. Swager, *Angew. Chem. Int. Ed.* **2012**, *51*, 5752–5756; *Angew. Chem.* **2012**, *124*, 5851–5855.
[17] M. Dionisio, J. M. Schnorr, V. K. Michaelis, R. G. Griffin, T. M. Swager, E. Dalcanale, *J. Am. Chem. Soc.* **2012**, *134*, 6540–6543.
[18] S. Santucci, S. Picozzi, F. Di Gregorio, L. Lozzi, C. Cantalini, L. Valentini, J. M. Kenny, B. Delley, *J. Chem. Phys.* **2003**, *119*, 10904–10910.
[19] D. Fu, H. Lim, Y. Shi, X. Dong, S. G. Mhaisalkar, Y. Chen, S. Moochhala, L. Li, *J. Phys. Chem. C* **2008**, *112*, 650–653.
[20] D. R. Kauffman, A. Star, *Angew. Chem. Int. Ed.* **2008**, *47*, 6550–6570; *Angew. Chem.* **2008**, *120*, 6652–6673.
[21] L. B. Da Silva, S. B. Fagan, R. Mota, *Nano Lett.* **2004**, *4*, 65–67.
[22] S. Peng, K. J. Cho, *Nano Lett.* **2003**, *3*, 513–517.
[23] Y. Wanna, N. Srisukhumbowornchai, A. Tuantranont, A. Wisitsoraat, N. Thavarungkul, P. Singjai, *J. Nanosci. Nanotechnol.* **2006**, *6*, 3893–3896.
[24] A. Star, V. Joshi, S. Skarupo, D. Thomas, J.-C. P. Gabriel, *J. Phys. Chem. B* **2006**, *110*, 21014–21020.
[25] O. K. Varghese, P. D. Kichambre, D. Gong, K. G. Ong, E. C. Dickey, C. A. Grimes, *Sens. Actuators B* **2001**, *81*, 32–41.
[26] S. Chopra, K. McGuire, N. Gothard, A. M. Rao, A. Pham, *Appl. Phys. Lett.* **2003**, *83*, 2280–2282.
[27] S. F. Liu, S. Lin, T. M. Swager, *ACS Sens.* **2016**, *1*, 354–357.
[28] X. Dong, D. Fu, M. O. Ahmed, Y. Shi, S. G. Mhaisalkar, S. Zhang, S. Moochhala, X. Ho, J. A. Rogers, L. J. Li, *Chem. Mater.* **2007**, *19*, 6059–6061.
[29] L. Que, W. B. Tolman, *Nature* **2008**, *455*, 333–340.
[30] W. B. Tolman, *Inorg. Chem.* **2013**, *52*, 7307–7310.
[31] M. C. De La Torre, M. A. Sierra, *Angew. Chem. Int. Ed.* **2004**, *43*, 160–181; *Angew. Chem.* **2004**, *116*, 162–184.
[32] S. J. Lippard, J. M. Berg, *Principles of Bioinorganic Chemistry*, University Science Books, Mill Valey, CA, **1994**.
[33] Y. He, J. Zhang, J. Zhao, *J. Phys. Chem. C* **2014**, *118*, 18325–18333.
[34] T. Shimizu, D. Huang, F. Yan, M. Stranava, M. Bartosova, V. Fojtíková, M. Martínková, *Chem. Rev.* **2015**, *115*, 6491–6533.
[35] M. He, T. M. Swager, *Chem. Mater.* **2016**, *28*, 8542–8549.
[36] S. Paul, F. Amalraj, S. Radhakrishnan, *Synth. Met.* **2009**, *159*, 1019–1023.
[37] W. Maser, E. M. Benito, E. Muñoz, M. T. Martinez, *Functionalized Nanoscale Materials, Devices and Systems*, Springer, Dordrecht, **2008**.
[38] S. Banerjee, T. Hemraj-Benny, S. S. Wong, *Adv. Mater.* **2005**, *17*, 17–29.
[39] L. Liu, K. C. Etika, K. S. Liao, L. A. Hess, D. E. Bergbreiter, J. C. Grunlan, *Macromol. Rapid Commun.* **2009**, *30*, 627–632.
[40] C. Rovira, P. Ballone, M. Parrinello, *Chem. Phys. Lett.* **1997**, *271*, 247–250.
[41] L. M. Blomberg, M. R. A. Blomberg, P. E. M. Siegbahn, *J. Inorg. Biochem.* **2005**, *99*, 949–958.
[42] A. Abdurahman, T. Renger, *J. Phys. Chem. A* **2009**, *113*, 9202–9206.
[43] J. A. Bailey, *J. Chem. Educ.* **2011**, *88*, 995–998.
[44] D. R. Kauffman, O. Kuzmych, A. Star, *J. Phys. Chem. C* **2007**, *111*, 3539–3543.
[45] G. Balducci, G. Chottard, C. Gueutin, D. Lexa, J.-M. Saveant, *Inorg. Chem.* **1994**, *33*, 1972–1978.
[46] Z. Zanolli, R. Leghrib, A. Felten, J. J. Pireaux, E. Llobet, J. C. Charlier, *ACS Nano* **2011**, *5*, 4592–4599.
[47] Q. Wang, Y. Tong, X. Xu, *Struct. Chem.* **2015**, *26*, 815–822.
[48] W. L. Yim, Z. F. Liu, *Chem. Phys. Lett.* **2004**, *398*, 297–303.
[49] M. Penza, M. Alvisi, R. Rossi, E. Serra, R. Paolesse, A. D'Amico, C. Di Natale, *Nanotechnology* **2011**, *22*, 125502.

Manuscript received: July 23, 2017
Revised manuscript received: August 16, 2017
Version of record online: October 4, 2017

